https://doi.org/10.3311/PPci.21620

Periodica Polytechnica Civil Engineering, 67(2), pp. 603–618, 2023

Mechanical Properties of Gas Storage Sandstone under Uniaxial Cyclic Loading and Unloading Condition

Zhao Baoyun[1*],·Wu Yingjie[1],·Yang Jiaosheng[2],·Sun Junchang[2], Huang Wei[1], Li Ziyun[1], Zhang Shuhan[1]

[1] School of Civil Engineering and Architecture, Chongqing University of Science and Technology, Chongqing 401331, China
[2] PetroChina Research Institute of Petroleum Exploration and Development, Beijing 100083, China
[*] Corresponding author, e-mail:

Received: 30 November 2022, Accepted: 23 February 2023, Published online: 06 March 2023

Abstract

In order to study the mechanical properties and damage evolution of the gas storage surrounding rock under the periodic injection-production process, the uniaxial cyclic loading and unloading tests of sandstone were carried out by TFD-2000 microcomputer servo-controlled rock triaxial testing machine. Results shown that the compressive strength of gas storage sandstone specimens were gradually decreases with increasing of the stress amplitude after 200 cycles. The stress-strain curve under uniaxial cyclic loading and unloading condition formed hysteresis loops, and the hysteresis loop presented sparse-dense-sparse when the stress amplitude was relative higher. The residual strains can be divided into three stages of decay deformation stage, stable deformation stage and accelerated deformation stage when the stress amplitude is 8~32 MPa, this phenomenon is very similar to the creep behavior of rocks. The energy evolution of sandstone under cyclic loading and unloading was analyzed and the damage evolution low of which was also discussed in detail, the damage variable defined by energy dissipative ratio accumulation can well reflect the damage development of sandstone under uniaxial cyclic loading and unloading. A nonlinear visco-plastic body was proposed by considering the accelerate stage of curves of the axial residual strains, and used the nonlinear visco-plastic body to replace the visco-plastic body of the traditional Nishihara model, a nonlinear viscoelastic-plastic model for cyclic loads was established and the applicability of the model is verified. The research results provide certain reference value for the construction and maintenance of gas storage.

Keywords

cyclic loading, energy evolution, energy dissipation, damage evolution, constitutive model

1 Introduction

In recent years, with the rapid development of economy and green energy, China's natural gas consumption has increased year by year. In order to ensure gas supply, China vigorously promotes the construction of underground gas storage. Frequent injection and production during operation of gas storage results in frequent changes of pressure in gas storage, resulting in fatigue stress, which will affect the mechanical properties of surrounding rock and the service life of gas storage [1]. Therefore, it is necessary to better understand the mechanical properties and damage evolution law of rock mass under fatigue state for the operation and maintenance of gas storage.

In the cyclic loading and unloading test, when the cumulative axial deformation of rock reaches the axial failure deformation of conventional test, rock failure occurs [2]. According to this characteristic, scholars deeply studied the fatigue life of rock, and found that after adding time interval in the fatigue process, the increase rate of axial deformation of rock was accelerated, resulting in the cumulative axial deformation of rock reaching the axial failure deformation under monotonic compression faster [3]. When studying the fatigue properties of rock, the cyclic loading and unloading method of axial stress is generally used for research. In the cyclic loading and unloading test, there are many factors affecting the strength of rock, such as loading frequency, temperature, stress amplitude, and cycle number [4–6]. These factors have different effects on the fatigue strength of rock. For example, the loading frequency has a significant deterioration effect on the fatigue strength of rock [4]. The increase of temperature also leads to the decrease of the fatigue strength of rock [5]. With the gradual deepening of the understanding of rock mechanical properties under fatigue loading, scholars began to study the development of internal

Cite this article as: Zhao, B., Wu, Y., Yang, J., Sun, J., Huang, W., Li, Z., Zhang, S. "Mechanical Properties of Gas Storage Sandstone under Uniaxial Cyclic Loading and Unloading Condition", Periodica Polytechnica Civil Engineering, 67(2), pp. 603–618, 2023. https://doi.org/10.3311/PPci.21620

damage of rocks under fatigue loading. In the process of cyclic loading and unloading, the surface of rock will produce cracks, and judging the internal damage development of rock by the crack volume is also a method adopted by many scholars at present [7–10]. This method can better reflect the damage state of the rock at various stages under fatigue loading, but the mechanism of the internal damage development of the rock is not clear enough. Regarding this problem, some scholars have begun to study the damage development in the rock under fatigue load from the energy point of view. Under fatigue loading, the internal energy of the rock is determined by the stress-strain curve. In the early research process, scholars used the internal elastic energy of the rock and the nature of the rock to determine the internal damage evolution trend of the rock under fatigue loading [11]. With the deepening of research, scholars have found that the deformation and failure of rocks during cyclic loading and unloading are always accompanied by energy dissipation. Based on this, scholars began to introduce the concept of dissipated energy to reflect the damage development of rock during cyclic loading and unloading through the accumulation of dissipated energy. [12–16].

With further research, scholars are not satisfied with only study the rock internal damage, began to build the constitutive model of rock under cyclic loading and unloading. Current research focuses on component model [17–21], damage fatigue constitutive model [22, 23] and empirical model [24]. The constitutive model that reflects the fatigue deformation of rock is established by combining the elastic, viscous and plastic body. Although the results are reliable, most of the component models adopt from the rheological model, and its physical meaning is not clear enough. At the same time, there is a certain controversy about the construction of the body of the instantaneous plastic strain. On the other hand, because the components of the component model are basic mechanical components, the component model describes the constitutive relationship of rock in uniaxial state, while the constitutive relationship of rock in triaxial state also needs to consider the influence of the deviatoric and spherical parts of the tensorial [25, 26]. The damage fatigue constitutive model constructs by introducing the damage variable and the stress equivalence principle, which mainly reflects the stress-strain curve of a certain cycle loading and unloading, and it is difficult to completely describe the whole process of rock cycle. Although, the constitutive model established according to the empirical formula can better reflect the changes of physical properties of rocks under cyclic loading and unloading, but the physical meaning of its parameters is not clear, it is not universally applicable.

In summary, scholars have made many achievements in the research area of mechanical properties, energy evolution, damage evolution trend and constitutive model construction of rocks under cyclic loading and unloading. However, as far as the current research status is concerned, the fatigue properties and damage evolution trend of sandstone in the four stages of deformation are still has certain research value. In this paper, the stress amplitude was determined by the four stages of sandstone deformation, and then the uniaxial cyclic loading and unloading test of sandstone was carried out. Based on the stress-strain relationship, the mechanical properties and energy evolution law of sandstone under fatigue load are analyzed, and the damage variable is constructed. By borrowing ideas from the rheological theory, a constitutive model which can reflect the deformation of sandstone under cyclic loading and unloading condition was constructed and the damage evolution trend of sandstone under fatigue load was determined, which provides a certain reference for the construction and maintenance of gas storage.

2 Materials and method

2.1 Specimen preparation

The natural sandstone used in the test was collected from a gas storage in Junggar, Xinjiang, China, which was a typical sandstone. First, a complete rock is obtained from about 3585 meters underground, then the rock core is obtained along the same direction of the rock, and finally the rock core is processed into a cylindrical solid standard sample with a height of 50 mm and a diameter of 25 mm (height-diameter ratio of 2:1) by indoor dry sawing, as shown in Fig. 1. The size of sandstone specimen is required to be processed in strict accordance with the ISRM test procedures, with the allowable error range of 0.3 mm in diameter and the non-parallelism of upper and lower end faces of 0.05 mm. The basic physical parameters of the specimens are shown in Table 1 and the average nature density of six specimens is around 2.44 g/cm^3, which is basically the same as the red sandstone specimens used by Gong et al. [27].

2.2 Testing equipment

The TFD-2000 microcomputer servo-controlled rock triaxial testing machine is adopted in the test as shown in Fig. 2. The maximum axial compressive force of the test

machine is 2000 kN and the pressure measurement error range is ±0.5%. During the test, the test data is automatically collected by microcomputer.

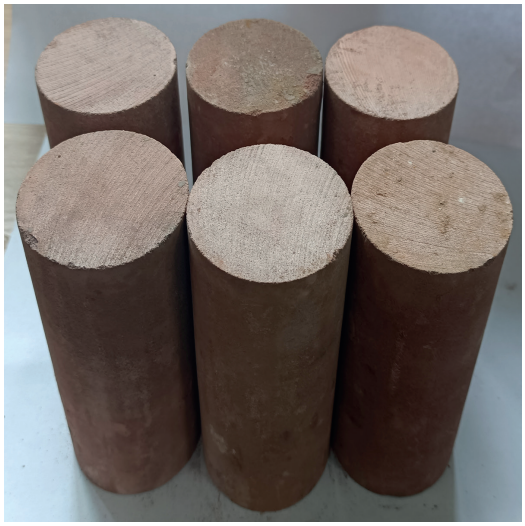

Fig. 1 Sandstone specimens

Table 1 Basic physical properties of the specimens

Specimen no.	Length (mm)	Diameter (mm)	Weight (g)	Density (g/cm^3)
A-1	51.10	25.30	63.93	2.49
A-2	50.54	25.30	62.73	2.47
A-3	50.40	24.95	60.83	2.47
D-1	50.10	24.98	58.41	2.38
D-2	50.80	25.10	61.05	2.43
D-3	50.18	25.05	59.32	2.4
Average	50.52	25.11	61.05	2.44

2.3 Preliminary test

Before the uniaxial cyclic loading and unloading test, the uniaxial compression tests of sandstone were conducted, the test results are shown in Table 2. It can be seen from Table 2 that the average uniaxial compressive strength (σ_c) of sandstone specimens is 42.76 MPa, the average peak axial strain (ε_{max}) is 5.1×10^{-3}, the average elastic modulus (E) is 9.53 GPa, and the average Poisson's ratio (v) is 0.21. Compared with the research results of Gong et al. [27], the peak axial strain and uniaxial peak strength of the red sandstone specimens used in this paper are slightly lower, which may be due to the relatively developed internal fractures of the specimens used in this paper. Fig. 3 shows the three uniaxial compressive stress-strain curves of sandstone specimens. It can be seen from Fig. 3(b) that the stress-strain curve of sandstone under uniaxial compression can be divided into four stages, namely, compaction stage (I), elastic stage (II), plastic stage (III) and failure stage (IV).

2.4 The cyclic loading and unloading test method

It can be also obtained from Fig. 3(b) that the stress level of specimens entered the elastic stage is about 8 MPa, and the average yield stress is about 24 MPa. So, in the cyclic

Table 2 The results of uniaxial compressive tests for sandstone specimens

Specimen no.	σ_c (MPa)	ε_{max} (10^{-3})	E (MPa)	v
A-1	41.69	5.24	9.74	0.20
A-2	43.65	4.62	9.38	0.22
A-3	42.95	5.45	9.47	0.21
Average	42.76	5.10	9.53	0.21

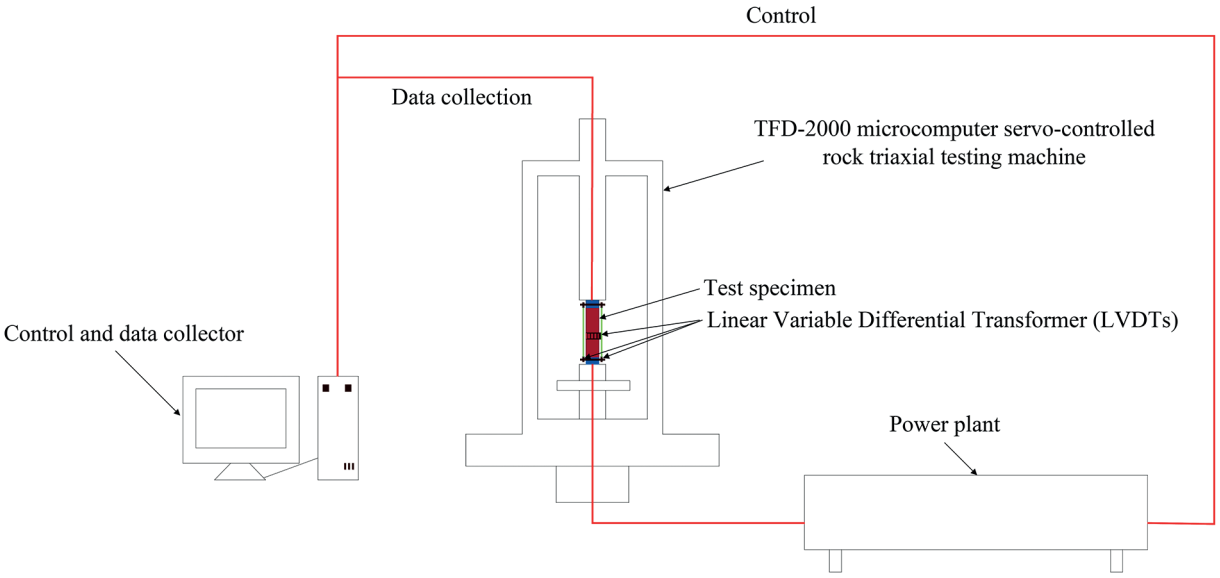

Fig. 2 The TFD-2000 microcomputer servo-controlled rock triaxial testing machine

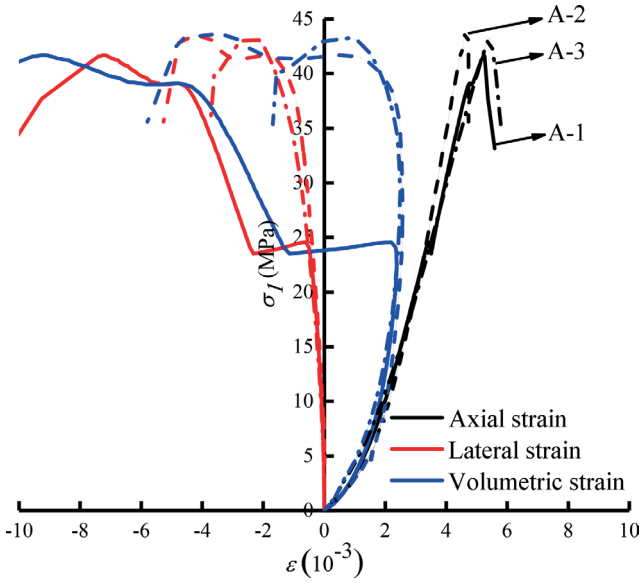

(a)

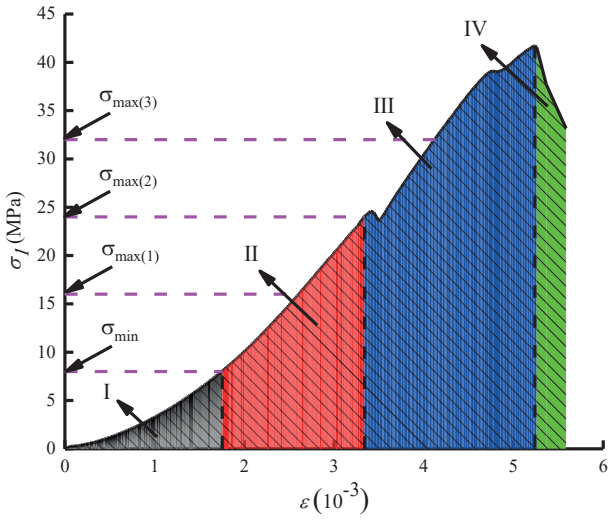

(b)

Fig. 3 The stress-strain curves under uniaxial compression tests; (a) The uniaxial compression stress-strain curve, (b) The four-stage diagram of uniaxial compression

loading and unloading tests, the stress value of 8 MPa was selected as cyclic lower limit stress σ_{min}, and the stress values of 16 MPa, 24 MPa and 32 MPa were as cyclic upper limit stress σ_{min}, the detailed test procedure as shown below:

Fist, the axial stress is loaded to the lower limit stress σ_{min} at a rate of 0.1 kN/s, and then apply the cyclic load at the speed of 0.2 kN/s, the stress path is from the lower limit stress σ_{min} to the upper limit stress σ_{max}, and then to the lower limit stress σ_{min}. After 200 cycles, a rate of 0.2 kN/s was selected again to apply axial stress until the specimen destroys. The detailed stress path as shown in Fig. 4 and the Table 3 present the upper limit stress value, lower limit stress value, cyclic stress amplitude, cycle number and loading frequency, respectively.

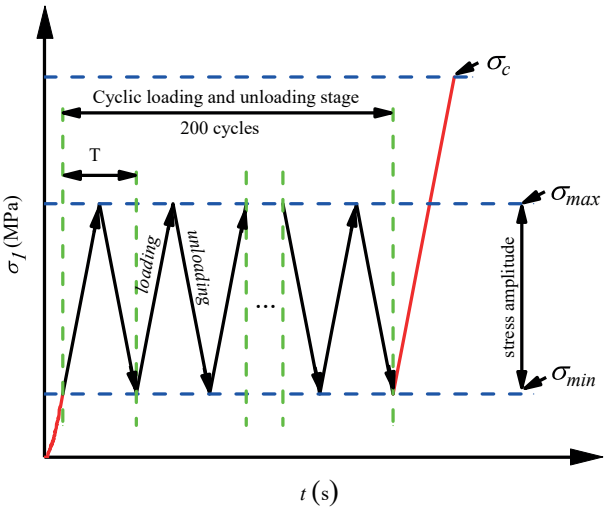

Fig. 4 Stress path diagram of cyclic loading and unloading test

Table 3 Uniaxial cyclic loading and unloading test procedure

Specimen no.	Upper limit stress (MPa)	Lower limit stress (MPa)	Cyclic stress amplitude (MPa)	Cycle Number (N)	Loading speed (kN/s)
D-1	16	8	8	200	0.2
D-2	24	8	16	200	0.2
D-3	32	8	24	200	0.2

3 Results and discussion

3.1 Mechanical properties of sandstone under cyclic loading and unloading

3.1.1 Deformation characteristics

Fig. 5(a)–(c) shows the stress-strain curves of sandstone under uniaxial cyclic loading and unloading tests with the stress amplitudes of 8–16 MPa, 8–24 MPa and 8–32 MPa, respectively. Fig. 6(a–c) shows the hysteresis loops of sandstone under different number of cycles with the stress amplitudes of 8–16 MPa, 8–24 MPa and 8–32 MPa, respectively.

Compare with Fig. 3(a), it can be seen that the stress-strain curve under uniaxial cyclic loading and unloading condition formed hysteresis loops, and the hysteresis loop presented sparse-dense-sparse when the stress amplitude was relative higher, means that the area of the hysteresis loop also presented development trend of large-small-large. It can be seen from Fig. 6 that the axial strain of sandstone specimens gradually increases with the increase of the number of cycles. When the stress amplitude was relative higher, the axial strain increases the most. It was found that the trend of the stress-strain curve of sandstone under cyclic loading was basically the same as that of sandstone under uniaxial compression before the beginning of cyclic loading, the stress-strain curve includes compaction stage (I) and elastic stage (II). While there was a certain value of permanent residual deformation after each

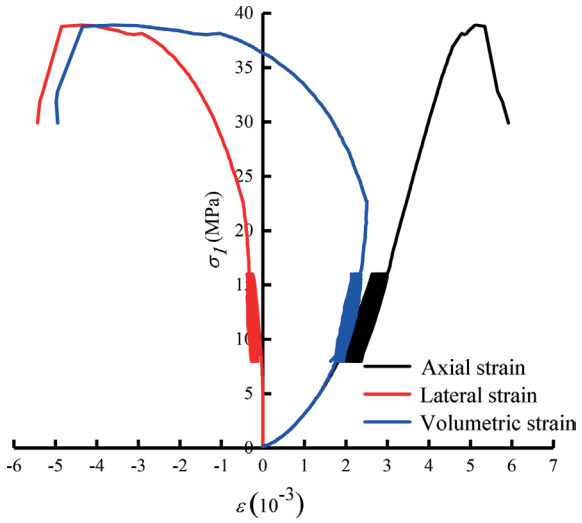

(a)

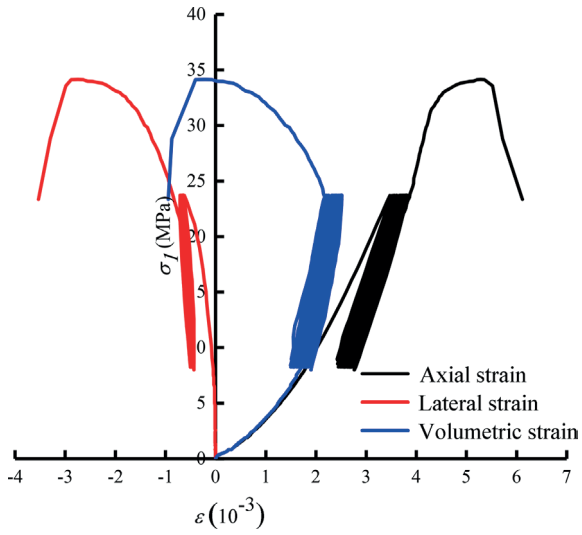

(b)

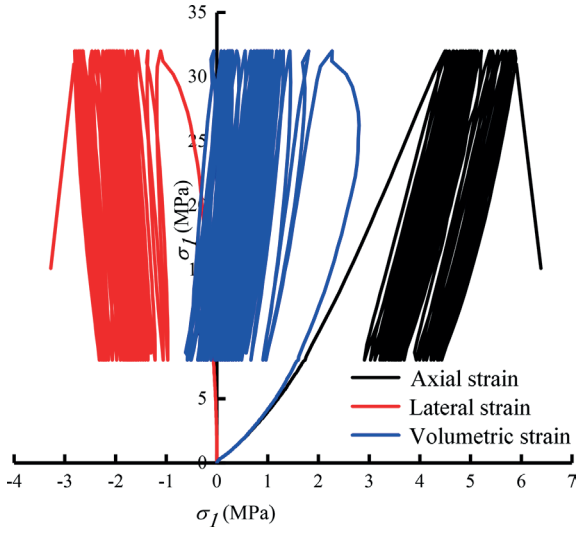

(c)

Fig. 5 The sandstone stress-strain curve under different stress amplitude; (a) D-1 (8-16 MPa), (b) D-2 (8-24 MPa), (c) D-3 (8-32MPa)

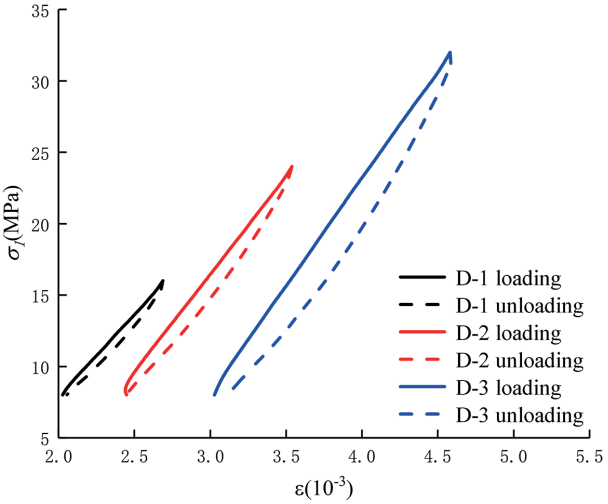

(a)

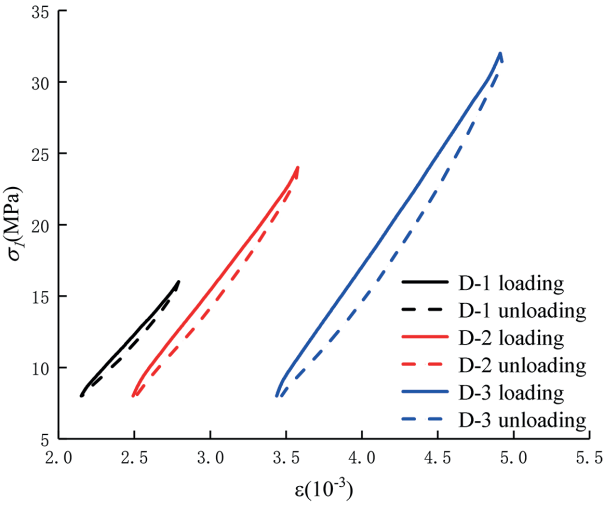

(b)

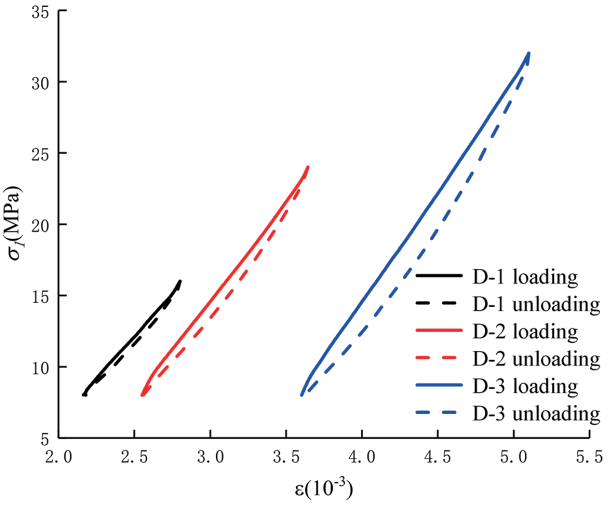

(c)

Fig. 6 The sandstone hysteresis loops under different number of cycles; (a) Cycle 2, (b) Cycle 10, (b) Cycle 20

cyclic loads, and then shape of the stress-strain curve was still similar with the uniaxial compression curve's when stress amplitude is relatively low. It can be also obtained that the stress-strain curves under cyclic loads are different in the failure stage, the stress of the sandstone under uniaxial compression drops rapidly, and the load capacity was lost in a short time, while the stress of the sandstone decreases relatively slow after cyclic loads and the axial strain increases rapidly as the loading progresses.

According to Fig. 5(a)–(c), it can be observed that the peak strength under cyclic loads were lower than the uniaxial compression tests and the uniaxial compressive strength gradually decreases with the increasing of the stress amplitude. When the stress amplitude was 8–16 MPa and 8–24 MPa, the peak stress of the specimen was 38.92 MPa and 34.13 MPa, respectively, which decreased by 9.3% and 20.4% compared with the peak stress under uniaxial compression. It was found that the sandstone is damaged after 31 cycles of loading and unloading condition when the stress amplitude is 8~32 MPa.

As we all know that the rock will form a hysteresis loop in the process of cyclic loading and unloading. In this paper, the axial strain at the point of lower limit stress was defined as the axial residual strain. The Fig. 7 shows the axial and radial residual strain evolution curve of sandstone under uniaxial cyclic loading and unloading, respectively. It can be observed from the Fig. 7 that the axial residual strain and radial residual strain gradually increases with the increasing of the cycles and stress amplitude. Integrating the curves of Fig. 7, it can be drawn that the curves of the residual strain rate versus cycles, as shown in Fig. 8. From Fig. 7 and Fig. 8, it can be easily

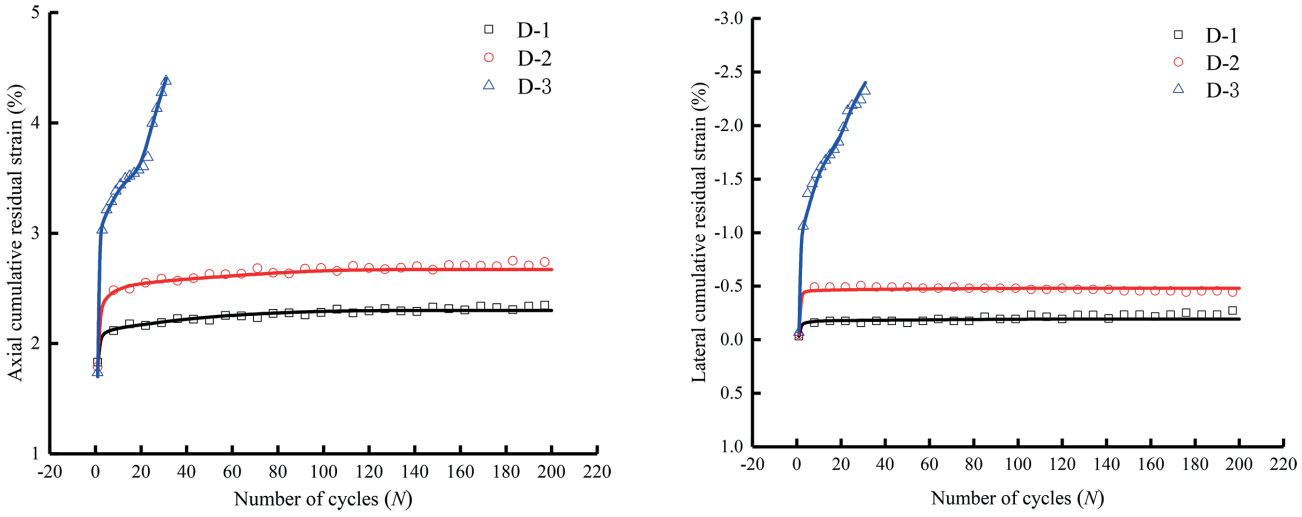

Fig. 7 The curves of the residual strains vs cycles; (a) Axial residual strain, (b) Lateral residual strain

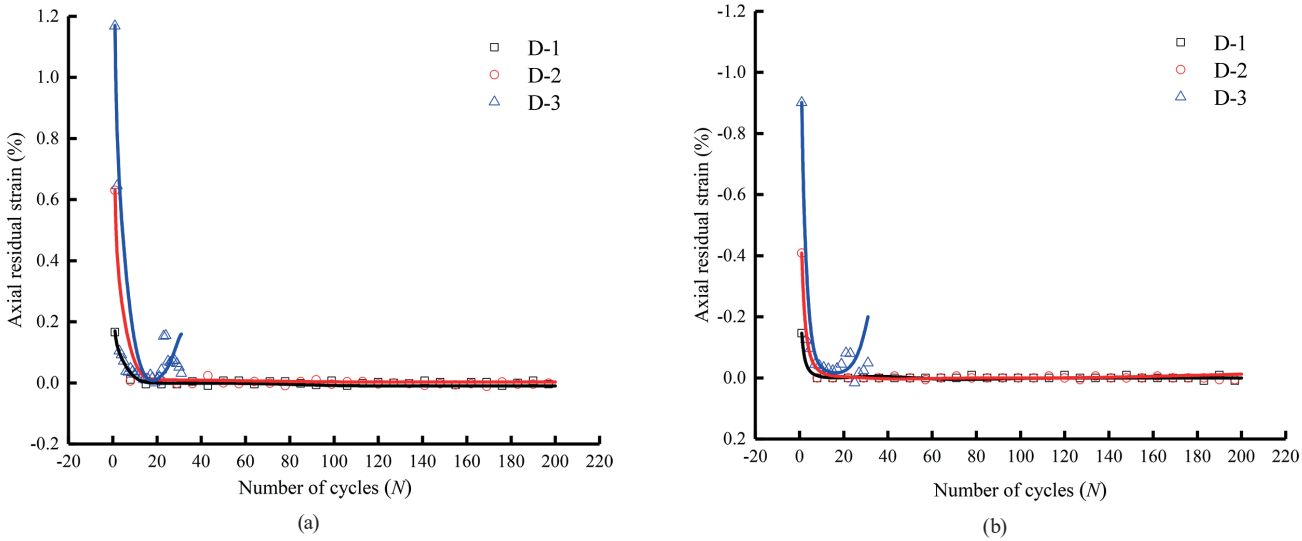

Fig. 8 The curves of the residual strain rate vs cycles; (a) Axial residual strain rate, (b) Lateral residual strain rate

concluded that the residual strains can be divided into two stages of decay deformation stage and stable deformation stage when stress amplitude is relatively low. While, the residual strains can be divided into three stages of decay deformation stage, stable deformation stage and accelerated deformation stage when the stress amplitude is 8~32 MPa. This phenomenon is very similar to the creep behavior of rocks.

3.1.2 The elastic modulus(*E*) and the Poisson's ratio(*μ*)

According to the Chinese Standard Test Procedure for Physical and Mechanical Properties of Rock Part 19, the elastic modulus and Poisson's ratio of rock under loading and unloading can be determined by the following Eqs. (1)–(4):

$$E_1 = \frac{\sigma_{\max} - \sigma_{\min}}{\varepsilon^l_{\max} - \varepsilon^l_{\min(1)}}, \tag{1}$$

$$E_2 = \frac{\sigma_{\max} - \sigma_{\min}}{\varepsilon^l_{\max} - \varepsilon^l_{\min(2)}}, \tag{2}$$

$$v_1 = \frac{\varepsilon^d_{\max} - \varepsilon^d_{\min(1)}}{\varepsilon^l_{\max} - \varepsilon^l_{\min(1)}}, \tag{3}$$

$$v_2 = \frac{\varepsilon^d_{\max} - \varepsilon^d_{\min(2)}}{\varepsilon^l_{\max} - \varepsilon^l_{\min(2)}}. \tag{4}$$

Where, E_1 is loaded modulus of elasticity, E_2 is unloading modulus of elasticity, v_1 is loading Poisson's ratio, v_2 is unloading Poisson's ratio, $\sigma_{\max}$ is maximum stress per cycle, $\sigma_{\min}$ is minimum stress per cycle, $\varepsilon^l_{\max}$ is maximum axial strain per cycle, $\varepsilon^l_{\min(1)}$ is minimum axial strain during loading, $\varepsilon^l_{\min(2)}$ is minimum axial strain during unloading, $\varepsilon^d_{\max}$ is maximum radial strain per cycle, $\varepsilon^d_{\min(1)}$ is minimum radial strain during loading, $\varepsilon^d_{\min(2)}$ is minimum radial strain during unloading. The calculation diagram of the elastic modulus and Poisson's ratio under cyclic loading and unloading condition as shown in Fig. 9.

The Fig. 10 shows the curves of the loading elastic modulus and Poisson's ratio versus cycles, and the curves of the unloading elastic modulus and Poisson's ratio versus cycles as shown in Fig. 11. It can be seen from Fig. 10 and Fig. 11 that the loading elastic modulus and the unloading Poisson's ratio present two stages of decaying and stabilizing, and there is an acceleration stage when the stress amplitude is largest. While, the unloading elastic modulus and the loading Poisson's ratio have the opposite

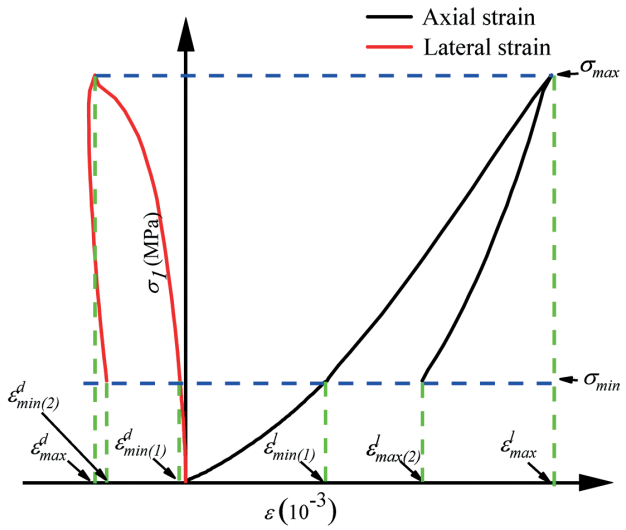

Fig. 9 The schematic diagram of loading and unloading elastic modulus and Poisson's ratio calculation

development trend, that is, the accelerated increase stage, the stability stage and the accelerated decay stage. It can be found that under the same stress amplitude, the unloading elastic modulus at the stable stage is slightly larger than the loading elastic modulus, while the unloading Poisson's ratio at the stable stage is slightly smaller than the loading Poisson's ratio. It can be found that the Poisson's ratio of loading and unloading is gradually approach, and the elastic modulus of loading and unloading is gradually approach with increasing of cycles. This is because, in the early cyclic stage, the internal microcracks of the rock specimen are compacted, resulting in a rapid increase in the elastic modulus and a decrease in the unloading elastic modulus. After that, the elastic deformation plays a dominant role resulting in a relatively stable loading and unloading elastic modulus. When the cyclic stress amplitude is largest, new micro-cracks appear and increasing with the cycle inside of the sandstone in the last few cycles, and the integrity of the sandstone is damaged, resulting in a rapid decline in the loading elastic modulus and an increase in the unloading elastic modulus. In the process of uniaxial cyclic loading and unloading, the radial deformation of the sample is not constrained. In the initial loading stage, the peak axial and radial deformation of sandstone increased rapidly and Poisson's ratio attenuates or increases. Later, the peak axial and radial deformation ratio of sandstone tends to be stable and Poisson's ratio tends to be relatively stable. In the last few cycles new cracks appear in the sample and the increase of radial deformation obviously leads to the rapid increase of the loading Poisson's ratio.

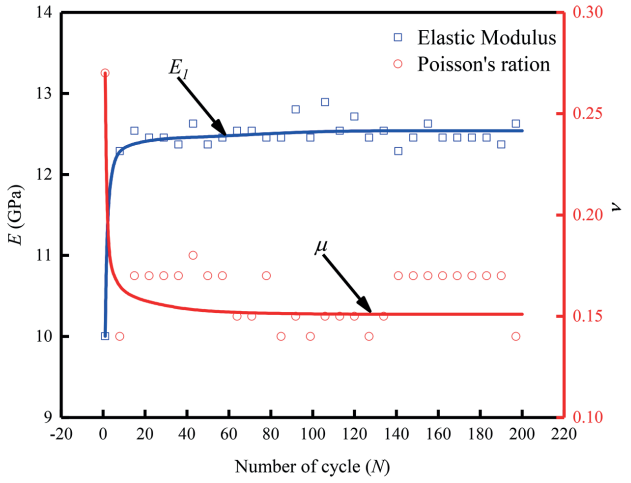

(a)

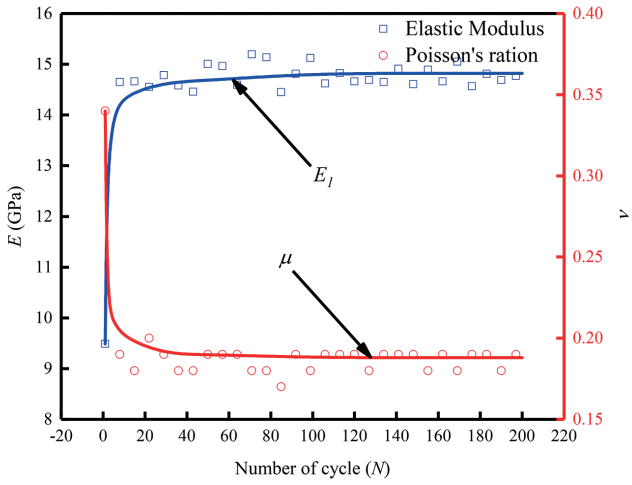

(b)

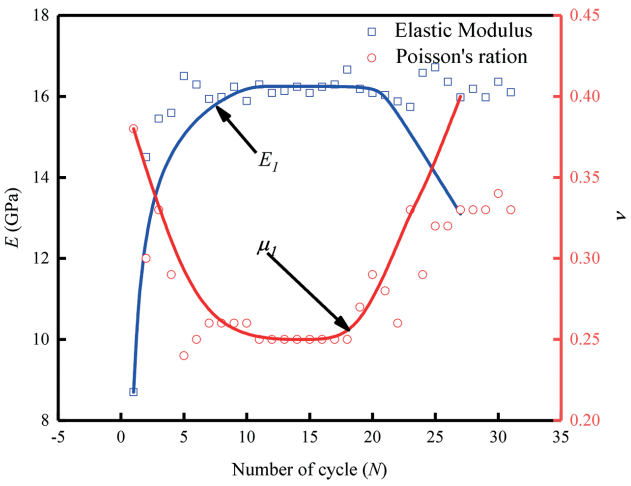

(c)

Fig. 10 The evolution curves of loading elastic modulus and Poisson's ratio of sandstone under different stress amplitudes; (a) D-1 (8-16 MPa), (b) D-2 (8-24 MPa), (c) D-3 (8-32 MPa)

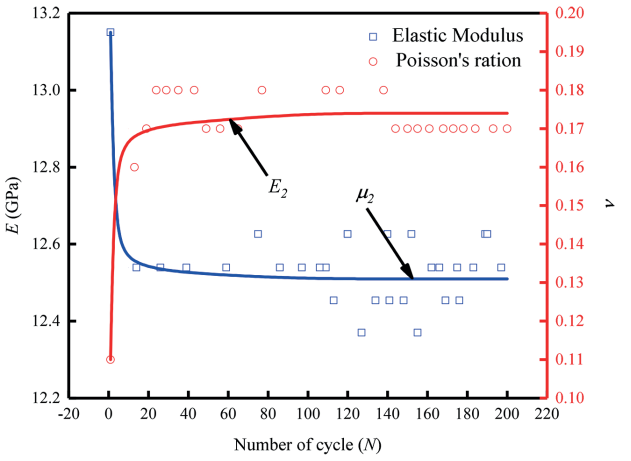

(a)

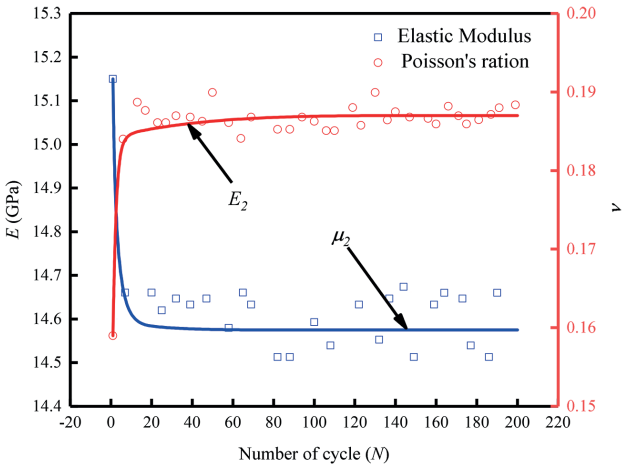

(b)

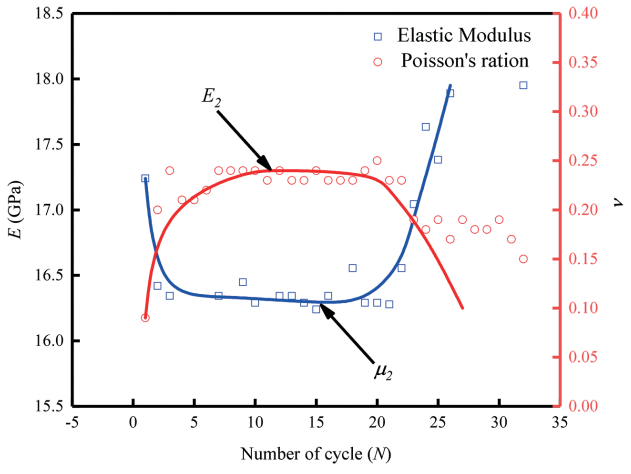

(c)

Fig. 11 The evolution curves of unloading elastic modulus and Poisson's ratio of sandstone under different stress amplitudes; (a) D-1 (8-16 MPa), (b) D-2 (8-24 MPa), (c) D-3 (8-32 MPa)

3.1.3 Failure mode

The failure mode diagram of sandstone under different stress amplitudes has seen in Fig. 12. It can be seen from the Fig. 12 that the failure mode form of sandstone in uniaxial compression test is mainly splitting failure which cracks penetrate the whole specimen, while the failure mode form of sandstone under uniaxial cyclic loading and unloading is splitting failure and accompanied by shear failure. It was also found that the damage under cyclic loading seems much more complete, the reason is that there are a large number of micro-fracture and volume expansion under the cyclic loading condition, which will also accompanied by a large number of local rupture or falling block phenomenon. And this phenomenon is even more obvious when the stress amplitude is higher.

3.2 Discuss of the energy and damage evolution

3.2.1 The energy evolution

External work is the main reason of rock failure during the process of the rock mechanics experiment [28]. Rock in the test process of cyclic loading and unloading, part of the energy is stored in the rock and the other part is dissipated. it is assumed that the total energy generated by the axial load in each cycle is U, as shown in Eq. (5):

$$U = U_m + U_w , \tag{5}$$

where, U_w is dissipation energy per cycle, U_m is elastic strain energy per cycle.

The schematic diagram of sandstone energy calculation under cyclic loading and unloading can be seen in Fig. 13. The elastic strain energy and dissipation energy of rocks can be calculated by stress-strain curves as shown in Eqs. (6)–(8) [29]:

$$U = \int_{\varepsilon^l_{\min(2)}}^{\varepsilon^l_{\max}} d\varepsilon \int_{\sigma_{\min}}^{\sigma_{\max}} f(\sigma_1) d\sigma , \tag{6}$$

$$U_m = \int_{\varepsilon^l_{\min(1)}}^{\varepsilon^l_{\max}} d\varepsilon \int_{\sigma_{\min}}^{\sigma_{\max}} f(\sigma_2) d\sigma , \tag{7}$$

$$U_w = U - U_m . \tag{8}$$

Where, $\sigma_{\max}$ is upper limit stress per cycle, $\sigma_{\min}$ is lower limit stress per cycle, $f(\sigma 1)$ is curve formula of each cycle loading segment, $f(\sigma 2)$ is curve formula of unloading section for each cycle, $\varepsilon_{\max}$ is maximum axial strain corresponding to the upper limit stress of each cycle, $\varepsilon_{\min(1)}$ is minimum axial strain corresponding to the lower limit stress of the loading section of each cycle, $\varepsilon_{\min(2)}$ is minimum axial strain corresponding to the lower limit stress of the unloading section of each cycle.

According to Eqs. (6)–(8), the energy of each cycle was calculated. Fig. 14 presents the energy evolution curve of sandstone under different stress amplitudes. It can be seen from Fig. 14 that energy evolution curves present the energy sudden drop stage and the energy stable stage when the stress amplitude was relatively small. While the energy

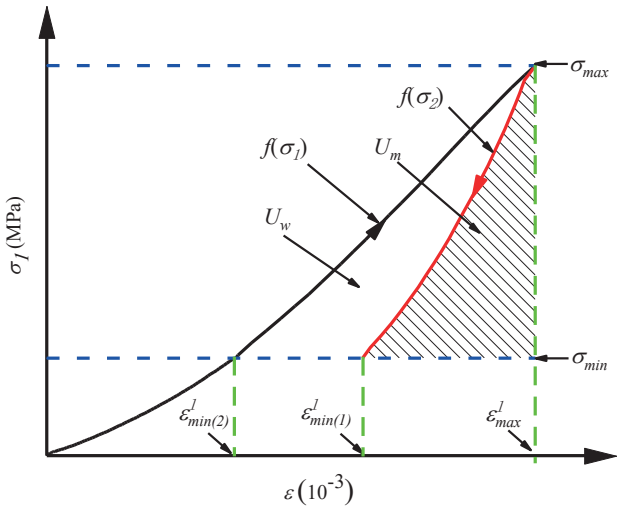

Fig. 13 The schematic diagram of sandstone energy calculation under cyclic loading and unloading condition

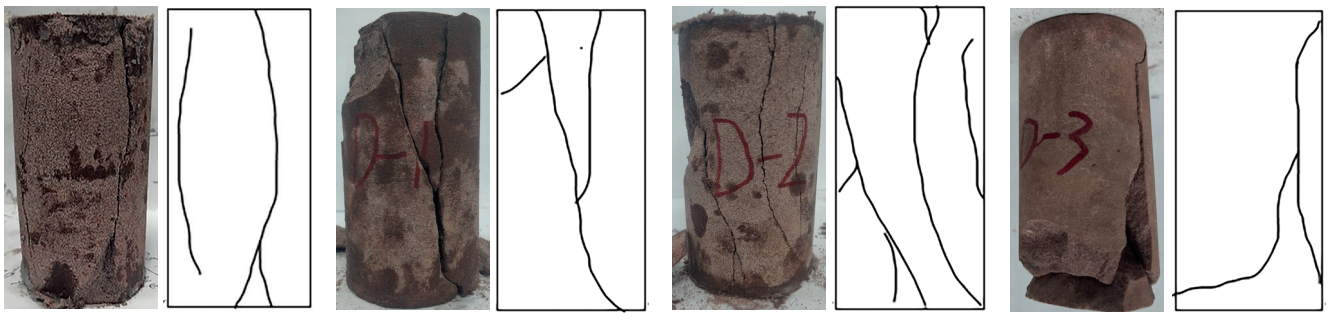

(a) (b) (c) (d)

Fig. 12 The failure mode of sandstone in uniaxial cyclic loading and unloading test; (a) Uniaxial compression, (b) D-1 (8-16 MPa), (c) D-2 (8-24 MPa), (d) D-3 (8-32 MPa)

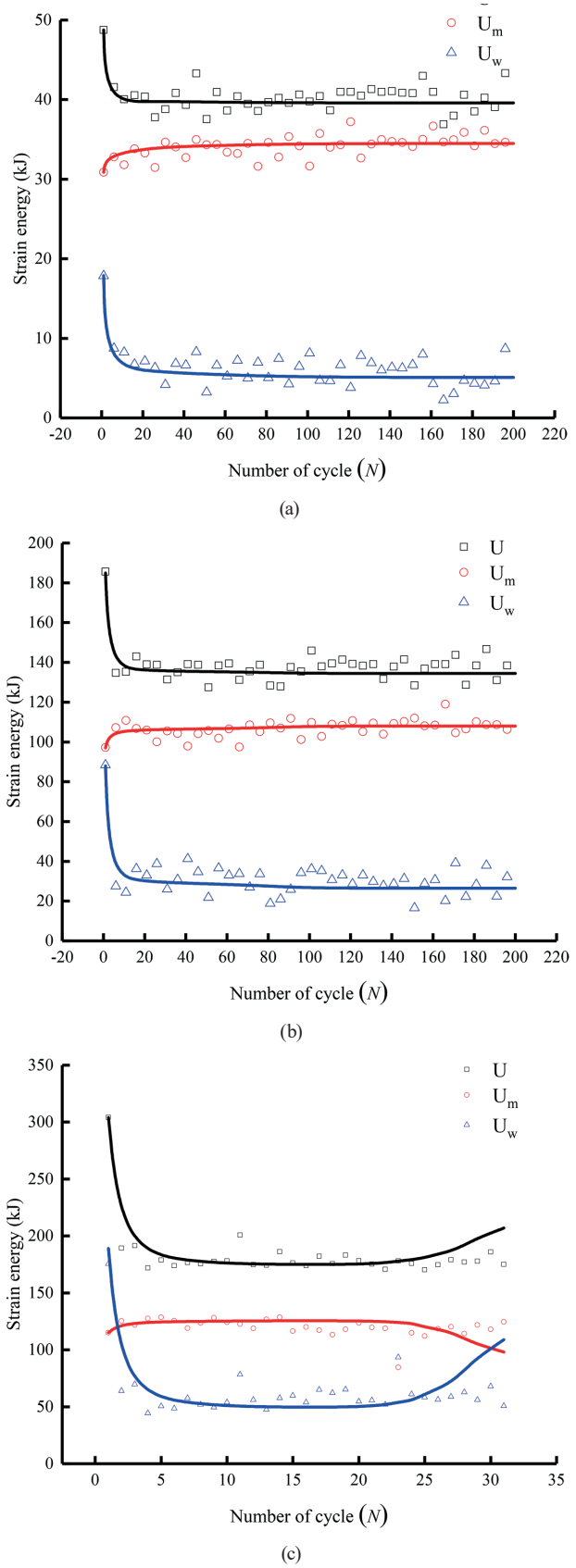

Fig. 14 The energy evolution curve of sandstone under different stress amplitude; (a) D-1 (8-16 MPa), (b) D-2 (8-24 MPa), (c) D-3 (8-32 MPa)

evolution can be divided into three stages: energy sudden drop stage, energy stabilization stage and energy accelerated increase stage when cyclic loading and unloading tests were carried out with the stress amplitude of 8–32 MPa. During the energy sudden drop stage, it was found that the total strain energy and dissipated energy of sandstone rapidly decrease, while the elastic energy increases, indicating that the energy absorbed by sandstone at this stage is mainly used for fracture compaction and increasing friction between particles. During the energy stabilization stage, all of the total energy, dissipated energy and elastic energy were tended to stable, indicating that the input energy at this stage is mainly stored in the specimen in the form of elastic energy, and results is the deformation of sandstone at this stage is mainly elastic deformation. During the energy accelerated increase stage, the total strain energy and dissipated energy were increasing with cycles, while the elastic energy was decreasing, indicating that the energy inside the sandstone begins to dissipate rapidly, and large cracks begin to appear inside the sandstone and the specimen enter the accelerated failure stage.

The variation trend of average dissipation energy on sandstone under different stress amplitudes can be seen in Fig. 15. With the increase of stress amplitude, the dissipation energy increases. The dissipation energy of 8–16 MPa stress amplitude is 373.93% lower than that of 8–24 MPa stress amplitude and 872.83% lower than that of 8–32 MPa stress amplitude. This shows that with the increase of the upper limit stress, the dissipation energy in sandstone increases exponentially and the damage development in sandstone accelerates.

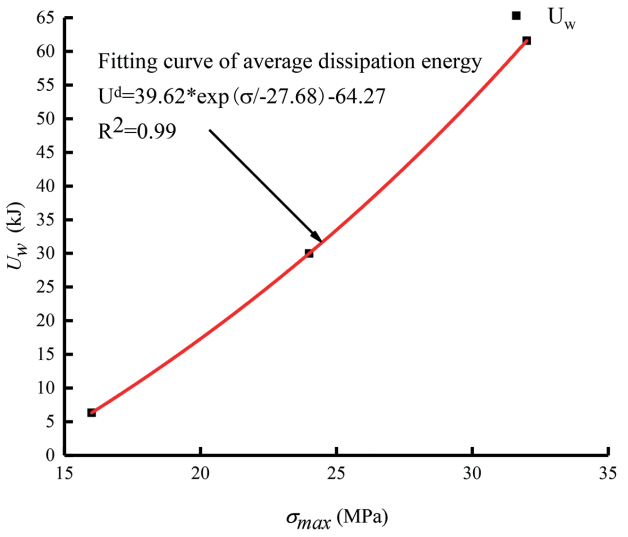

Fig. 15 The trend chart of average dissipated energy of sandstone under different stress amplitudes

The energy dissipation ratio (η) is the ratio of dissipated energy to total input energy, which can reflect the damage inside the rock during the cycle. The calculation formula is as shown in Eq. (9):

$$\eta = \frac{U_w}{U}. \tag{9}$$

According to Eq. (9), the evolution curves of energy consumption ratio of sandstone under different stress amplitudes can be calculated, as shown in Fig. 16.

The variation trend of internal energy dissipation ratio of sandstone under different stress amplitudes tends to be consistent, which is shown in Fig. 16. The energy dissipation ratio decreases rapidly by the initial cycle, and most of the total energy dissipation is absorbed by the rock in the initial cycle to compress the microcracks inside the rock. The energy dissipation ratio decreases with increasing number of cycles, internal cracks are compacted and dissipated energy decreases by rock under cyclic loading. The energy consumption ratio rises suddenly before rock is destroyed, this phenomenon shown that the development of new cracks in rock leads to further increase of damage, and then rock unstable failure.

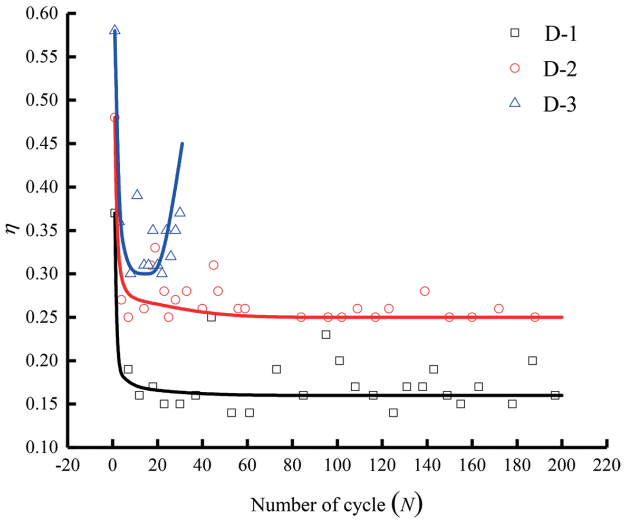

Fig. 16 The evolution curve of energy dissipation ratio of sandstone under different stress amplitudes

3.2.2 Damage evolution law

The current research shows that the energy dissipation of rock comes from the damage of rock, and the damage is related to the energy dissipation, so scholars begin to define the damage variable of rock based on the energy dissipation. In this paper, taking the dissipation energy at the beginning of the cycle as the initial damage point and the total dissipation energy at the end of the cycle as the damage point, the damage variable can be defined as shown in Eq. (10) [14, 29]:

$$D_i = \frac{\sum_i^N U_w}{U_{w1}}, \tag{10}$$

where, N is total number of cycles, i is a cycle, D_i is damage variable of the i cycle, U_{w1} is total energy dissipation.

The energy damage of sandstone under different stress amplitudes is calculated by Eq. (10). Fig. 17 shows the evolution law of energy damage of sandstone under different stress amplitudes.

The diagram of the evolution law of sandstone energy damage under different stress amplitudes in Fig. 17. When the number of cycles increases, there are obvious nonlinear relationship between the energy damage variable and the axial strain of sandstone. The energy damage evolution can be divided into three stages under 8–32 MPa stress amplitude: the accumulation rate of damage slowly rising in elastic stage, and the accumulation rate of damage sudden increase when the plastic stage. In the failure stage, the damage keeps accumulating at a high speed, and the axial strain is close to the failure strain when the sandstone specimen is completely broken is shown in Fig. 17(c). The damage variable evolution curve is 'S' type line in the whole cycle process. The upper loading stress is less than the yield strength when the 8–16 MPa stress are amplitude and 8–24 MPa amplitude, so the accumulation rate of energy damage rises slowly at the beginning of the cycle and then rises rapidly after the end of the cycle.

4 Constitutive model

The above-mentioned deformation characteristics of sandstone under cyclic loading and unloading condition shown that the curves of the residual strain can be divide into decay deformation stage and stable deformation stage under low stress amplitude, while the curve of sandstone experienced rapid rise in the early stage, stable in the middle stage, and accelerate rise stage under high stress amplitude, which is similar very to the rheological curve of sandstone. So, it is feasible to introduce a rheological model to describe the fatigue deformation. However, the rheological time and the cycles are two different dimensional physical variables, therefore, it is necessary to improve the rheological model to accurately describe the development trend of rock residual deformation in fatigue test.

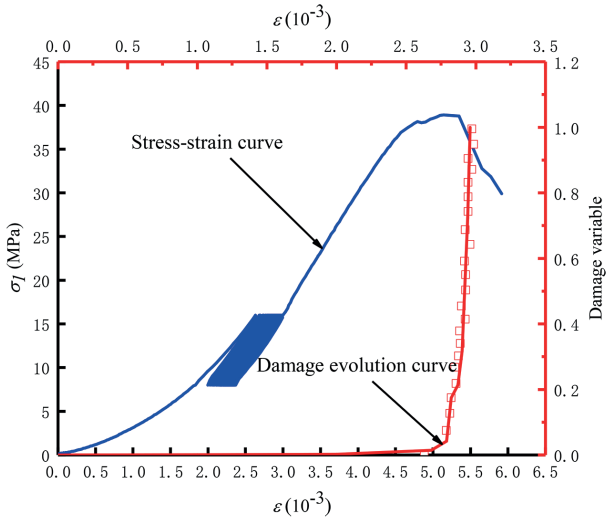

(a)

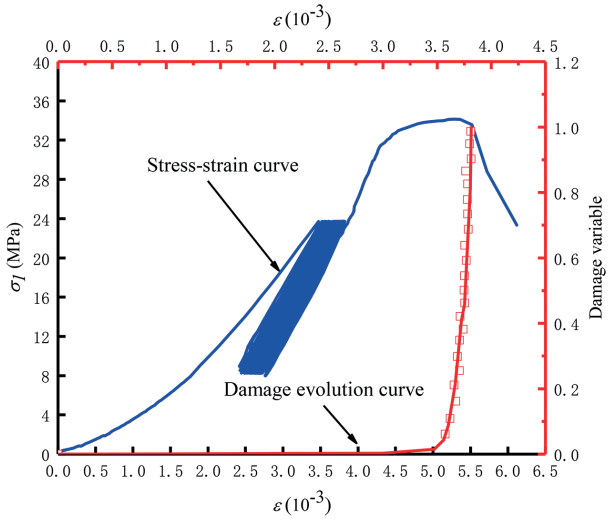

(b)

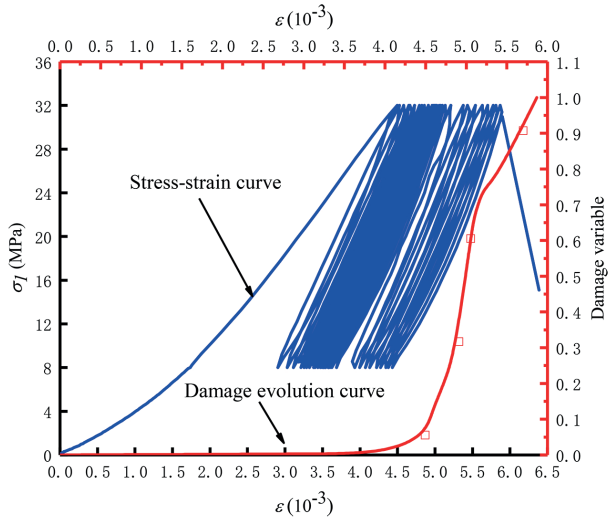

(c)

Fig. 17 The diagram of the evolution law of sandstone energy damage under different stress amplitudes;
(a) D-1 (8-16 MPa), (b) D-2 (8-24 MPa), (c) D-3 (8-32 MPa)

4.1 Construction of constitutive model

4.1.1 Stress equivalent

As the loading wave of this cyclic loading and unloading test is triangular wave, which belongs to a complex stress loading mode, according to the rheological theory, the equivalent stress σ_N of this test is calculated according to Eq. (11) [30]:

$$\begin{cases} \sigma_N = \left(\dfrac{\sigma_{\max}+\sigma_{\min}}{2}\right) e^{\left(\frac{\sigma_{\max}-\sigma_s}{\sigma_c}\right) f} \\ f = \dfrac{1}{T} \end{cases}, \tag{11}$$

where, σ_s is failure stress, f is period frequency, T is the loading and unloading period.

4.1.2 Nonlinear visco-plastic body

As we all known that the five element the traditional Nishihara model cannot fully describe the whole creep stage due to the linear characteristics of each element. Consider this feature in depth and take the accelerate stage of curves of the D-1 axial residual strains versus cycles as the research object, it was found that a power function can be used to describe this curve as shown in Fig. 18 [31].

Fitting of accelerated deformation curve of sandstone under cyclic loading and unloading, a power function can be expressed as Eq. (12):

$$\varepsilon = \varepsilon_0 + AN^n, \tag{12}$$

where, ε_0 is strain during the first cycle, A is fitting parameters, N is cycle number, n is accelerated deformation parameters.

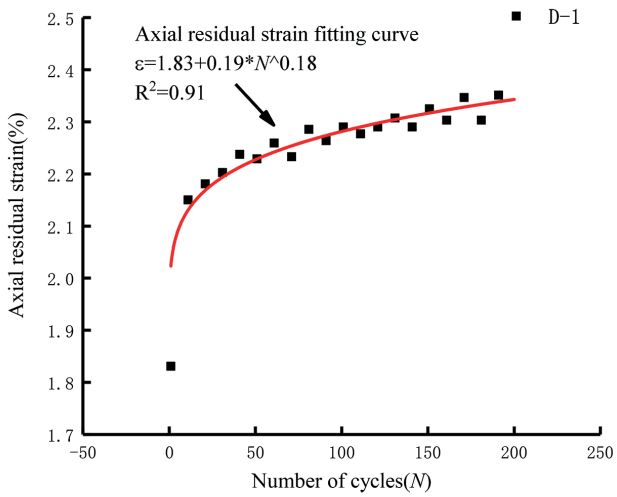

Fig. 18 The accelerate stage of curves of the axial residual strains versus cycles

It is known that the function of ideal viscous element is Eq. (13):

$$\varepsilon = \frac{\sigma}{\eta} t + \varepsilon_0 , \tag{13}$$

where, η is viscosity coefficient of sandstone.

For the deformation evolution of sandstone under cyclic loading and unloading condition as shown in Fig. 7, the time t in ideal viscous element can be modified as N/f. So, According to Eqs. (12) and (13), a nonlinear viscous body is proposed, and the nonlinear parameter η can be expressed as Eq. (14):

$$\eta(N,n) = \frac{\sigma}{AN^{n-1} f} . \tag{14}$$

4.1.3 Establish of the constitutive model

By using the proposed nonlinear visco-plastic body to replace the visco-plastic body of the traditional Nishihara mode, and redefine each element meaning of the mode to meet to the cyclic load deformation characteristics, a nonlinear viscoelastic-plastic model for cyclic loads was established as shown in Fig. 19 [32].

It can be easily obtained from Fig. 19 that when the equivalent cyclic stress σ_N is less than the failure stress σ_{aN}, the total strain is equal to ε_1 add ε_2. While the total strain is equal to ε_1 add ε_2 add ε_3 when the equivalent cyclic stress σ_N is larger than the failure stress σ_{aN}. Based on the rheological mechanics theory, when the body are paralleled, the stress is added and the strain is equal. When the body are in series, the stress is equal, and the strain is added. Then the differential equation of the nonlinear viscoelastic-plastic model can be expressed as Eqs. (15) and (16):

$$\begin{cases} \sigma_{1N} = \varepsilon_1 \mathrm{E}_{1N} \\ \sigma_{2N} = \varepsilon_2 E_{2N} + \eta_{1N} \dfrac{d\varepsilon_2}{dN} f \quad (\sigma_N < \sigma_{aN}) \\ \varepsilon = \varepsilon_1 + \varepsilon_2 \\ \sigma_N = \sigma_{1N} = \sigma_{2N} \end{cases}, \tag{15}$$

$$\begin{cases} \sigma_{1N} = \varepsilon_1 E_{1N} \\ \sigma_{2N} = \varepsilon_2 E_{2N} + \eta_{1N} \dfrac{d\varepsilon_2}{dN} f \\ \sigma_{3N} = \sigma_{aN} + \eta(N,n) \dfrac{d\varepsilon_3}{dN} f \quad \sigma_N \geq \sigma_{aN} \\ \varepsilon = \varepsilon_1 + \varepsilon_2 + \varepsilon_3 \\ \sigma_N = \sigma_{1N} = \sigma_{2N} = \sigma_{3N} \end{cases} . \tag{16}$$

Where, σ_{aN} is failure stress under cyclic loading and unloading condition, σ_N is equivalent cyclic stress. E_{1N} and E_{2N} are the cyclic elastic modulus, respectively. η_{1N} is the viscous coefficient of rock under fatigue state.

According to Eqs. (14), (15) and (16), the nonlinear viscoelastic plastic model of sandstone under uniaxial cyclic loading and unloading can be expressed as Eq. (17):

$$\begin{cases} \varepsilon = \dfrac{\sigma_N}{E_{1N}} + \dfrac{\sigma_N}{E_{2N}} \left[1 - e^{-\frac{E_{2N}}{\eta_1} \frac{N}{f})} \right] & (\sigma_N < \sigma_{aN}) \\ \varepsilon = \dfrac{\sigma_N}{E_{1N}} + \dfrac{\sigma_N}{E_{2N}} \left[1 - e^{-\frac{E_{2N}}{\eta_1} \frac{N}{f})} \right] + \dfrac{(\sigma_N) N^n A}{\sigma} & (\sigma_N \geq \sigma_{aN}) \end{cases} . \tag{17}$$

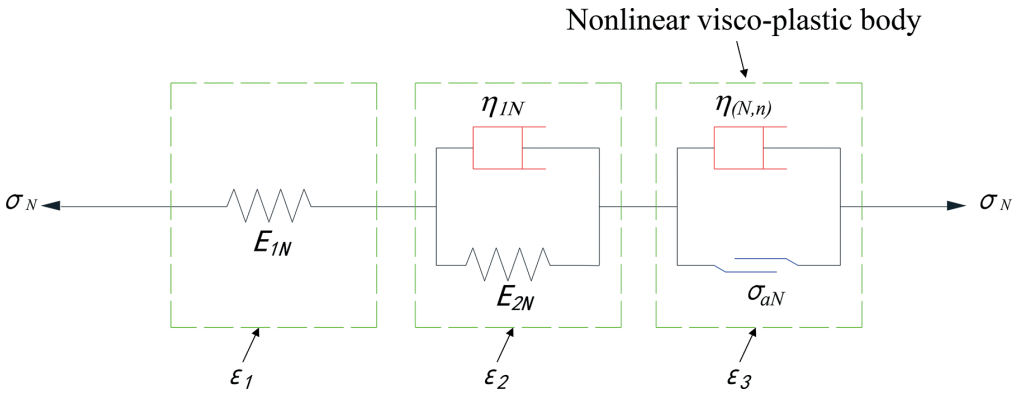

Fig. 19 The nonlinear viscoelastic-plastic model

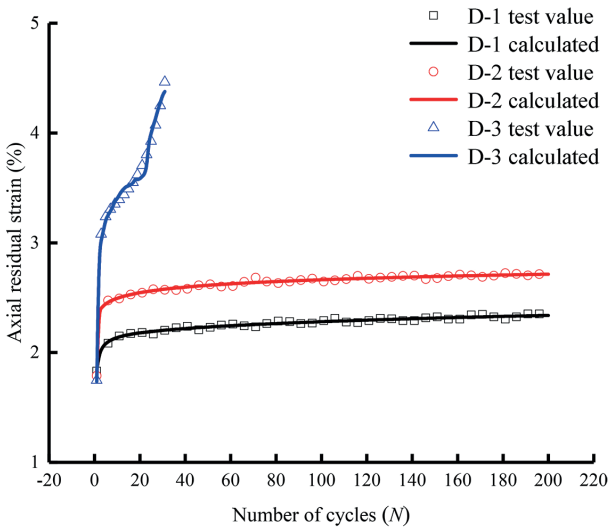

Fig. 20 Theoretical and test curves under different stress amplitude

4.2 Verification of model

According to Eqs. (11) and (17), the data calculated by the nonlinear viscoelastic-plastic model were used to compared with the test results as shown in Fig. 7 (a), as shown in Fig. 20. It can be seen from Fig. 20 that the proposed nonlinear viscoelastic-plastic model in this paper is in good agreement with the test results illustrate that the nonlinear viscoelastic-plastic model can better reflect the whole residual deformation of sandstone under cyclic loading and unloading, and the applicability of the model is verified.

5 Conclusions

In order to study the mechanical properties of sandstone under uniaxial cyclic loading and unloading condition, the uniaxial cyclic loading and unloading tests with different stress amplitudes of gas storage sandstone were carried out. From the test results, the following conclusions can be drawn:

(1) The stress-strain curve under uniaxial cyclic loading and unloading condition formed hysteresis loops, and the hysteresis loop presented sparse-dense-sparse when the stress amplitude is 8–32 MPa. The compressive strength of gas storage sandstone specimens was gradually decreases with increasing of the stress amplitude after 200 cycles.

(2) The axial deformation and radial deformation of sandstone can be divided into three stages of decay deformation stage, stable deformation stage and accelerated deformation stage when the stress amplitude is 8–32 MPa. There are decay deformation stage and stable deformation stage when the stress amplitude is 8–16 MPa, 8–24 MPa. These phenomena are very similar to the creep behavior of rocks. And the elastic modulus and energy have similar characteristics.

(3) It is a good way to define damage variable based on energy evolution, the damage variable defined by energy dissipative ratio accumulation can well reflect the damage development of sandstone under uniaxial cyclic loading and unloading.

(4) A nonlinear viscoelastic-plastic model for cyclic loads was established by redefining the meaning of each parameter and using the nonlinear visco-plastic body to replace the visco-plastic body of the traditional Nishihara model. The applicability of the nonlinear viscoelastic-plastic model was also verified.

Acknowledgements

The project presented in this article is supported by the National Natural Science Foundation of China (Grant No.41302223). The Natural Science Foundation of Chongqing (No. cstc2020jcyj-msxmX0567; No. cstc-2020jcyj-msxmX0558). Scientific and Technological Research Program of Chongqing Municipal Education Commission (KJZD-K202101505). Chongqing University of Science and Technology Graduate Students' Science and Technology Innovation Program (YKJCX2020653, YKJCX2120658).

Declarations

Data availability

The data used to support the findings of this study are included within the article.

Conflict of interest

The authors declare no competing interest.

References

[1] Wang, Z., Li, W., Qiao, L., Guo, J., Liu, Y. "Effects of rate-dependent behavior of sandstone on performance of gas storage in aquifer", Geomechanics for Energy and the Environment, 31, 100262, 2021. https://doi.org/10.1016/j.gete.2021.100262

[2] Xu, T., Fu, M., Yang, S., Heap, M. J., Zhou, G. "A numerical meso-scale elasto-plastic damage model for modeling the deformation and fracturing of sandstone under cyclic loading", Rock Mechanics and Rock Engineering, 54(9), pp. 4569–4591, 2021. https://doi.org/10.1007/s00603-021-02556-2

[3] Fan, J., Jiang, D., Liu, W., Wu, F., Chen, J., Daemen, J. J. K. "Discontinuous fatigue of salt rock with low-stress intervals", International Journal of Rock Mechanics and Mining Sciences, 115, pp. 77–86, 2019. https://doi.org/10.1016/j.ijrmms.2019.01.013

[4] Arora, K., Chakraborty, T., Rao, K. S. "Experimental study on stiffness degradation of rock under uniaxial cyclic sinusoidal compression loading", Rock Mechanics and Rock Engineering, 52(11), pp. 4785–4797, 2019. https://doi.org/10.1007/s00603-019-01835-3

[5] Meng, Q., Liu, J., Pu, H., Yu, L., Wu, J., Wang, C. "Mechanical properties of limestone after high-temperature treatment under triaxial cyclic loading and unloading conditions", Rock Mechanics and Rock Engineering, 54, pp. 6413–6437, 2021. https://doi.org/10.1007/s00603-021-02638-1

[6] Xiao, F., Jiang, D., Wu, F., Zou, Q., Chen, J., Chen, B., Sun, Z. "Effects of prior cyclic loading damage on failure characteristics of sandstone under true-triaxial unloading conditions", International Journal of Rock Mechanics and Mining Sciences, 132, 104379, 2020. https://doi.org/10.1016/j.ijrmms.2020.104379

[7] Wang, Y., Feng, W. K., Hu, R. L., Li, C. H. "Fracture evolution and energy characteristics during marble failure under triaxial fatigue cyclic and confining pressure unloading (FC-CPU) conditions", Rock Mechanics and Rock Engineering, 54(2), pp. 799–818, 2020. https://doi.org/10.1007/s00603-020-02299-6

[8] Zhou, Y., Zhao, D., Li, B., Wang, H., Zhang, Z. "Fatigue damage mechanism and deformation behaviour of granite under ultra-high-frequency cyclic loading conditions", Rock Mechanics and Rock Engineering, 54(9), pp. 4723–4739, 2021. https://doi.org/10.1007/s00603-021-02524-w

[9] Ghasemi, S., Khamehchiyan, M., Taheri, A., Nikudel, M. R., Zalooli, A. "Microcracking behavior of gabbro during monotonic and cyclic loading", Rock Mechanics and Rock Engineering, 54(5), pp. 2441–2463, 2021. https://doi.org/10.1007/s00603-021-02381-7

[10] Chen, Y., Guo, W., Zuo, J., Heng, S., Dou, R. "Effect of triaxial loading and unloading on crack propagation and damage behaviors of sandstone: an experimental study", Rock Mechanics and Rock Engineering, 54, pp. 6077–6090, 2021. https://doi.org/10.1007/s00603-021-02605-w

[11] Peng, R., Xie, H., Ju, Y. "Analysis of energy dissipation and damage evolution of sandstone during tensile process", Chinese Journal of Rock Mechanics and Engineering, 26(12), pp. 2526–2531, 2007. https://doi.org/10.3321/j.issn:1000-6915.2007.12.019

[12] Zhou, Y., Sheng, Q., Li, N., Fu, X. "The influence of strain rate on the energy characteristics and damage evolution of rock materials under dynamic uniaxial compression", Rock Mechanics and Rock Engineering, 53(8), pp. 3823–3834, 2020. https://doi.org/10.1007/s00603-020-02128-w

[13] Li, T., Pei, X., Guo, J., Meng, M., Huang, R. "An energy-based fatigue damage model for sandstone subjected to cyclic loading", Rock Mechanics and Rock Engineering, 53, pp. 5069–5079, 2020. https://doi.org/10.1007/s00603-020-02209-w

[14] Bagde, M. N., Petroš, V. "Fatigue and dynamic energy behaviour of rock subjected to cyclical loading", International Journal of Rock Mechanics and Mining Sciences, 46(1), pp. 200–209, 2009. https://doi.org/10.1016/j.ijrmms.2008.05.002

[15] Steffler, E. D., Epstein, J. S., Conley, E. G. "Energy partitioning for a crack under remote shear and compression", International Journal of Fracture, 120(4), pp. 563–580, 2003. https://doi.org/10.1023/A:1025511703698

[16] Gong, F., Zhang, P., Du, K. "A Novel Staged Cyclic Damage Constitutive Model for Brittle Rock Based on Linear Energy Dissipation Law: Modelling and Validation", Rock Mechanics and Rock Engineering, 55(10), pp. 6249–6262, 2022. https://doi.org/10.1007/s00603-022-02930-8

[17] Liu, J., Pu, S., Rao, J. "Visco-elastoplastic constitutive fatigue model for rocks", Advances in Civil Engineering, 2020, 4292043, 2020. https://doi.org/10.1155/2020/4292043

[18] Lyu, C., Liu, J., Ren, Y., Chao, L., Liao, Y. "Study on very long-term creep tests and nonlinear creep-damage constitutive model of salt rock", International Journal of Rock Mechanics and Mining Sciences, 146, 104873, 2021. https://doi.org/10.1016/j.ijrmms.2021.104873

[19] Liu, Y., Dai, F. "A damage constitutive model for intermittent jointed rocks under cyclic uniaxial compression", International Journal of Rock Mechanics and Mining Sciences, 103, pp. 289–301, 2018. https://doi.org/10.1016/j.ijrmms.2018.01.046

[20] Matsuki, K., Takeuchi, K. "Three-dimensional in situ stress determination by anelastic strain recovery of a rock core", International Journal of Rock Mechanics and Mining Sciences & Geomechanics Abstracts, 30(7), pp. 1019–1022, 1993. https://doi.org/10.1016/0148-9062(93)90064-K

[21] Matsuki, K. "Anelastic strain recovery compliance of rocks and its application to in situ stress measurement", International Journal of Rock Mechanics and Mining Sciences, 45(6), pp. 952–965, 2008. https://doi.org/10.1016/j.ijrmms.2007.10.005

[22] He, M., Li, N., Zhu, C., Chen, Y., Wu, H. "Experimental investigation and damage modeling of salt rock subjected to fatigue loading", International Journal of Rock Mechanics and Mining Sciences, 114, pp. 17–23, 2019. https://doi.org/10.1016/j.ijrmms.2018.12.015

[23] Zhu, Y., Yu, J., Cai, Y., Tang, X., Yao, W., Liu, X. "A novel fatigue damage model of rock considering temperature effects", Advances in Civil Engineering, 2020, 8838335, 2020. https://doi.org/10.1155/2020/8838335

[24] Li, P., Cai, M. "Energy evolution mechanism and failure criteria of jointed surrounding rock under uniaxial compression", Journal of Central South University, 28(6), pp. 1857–1874, 2021. https://doi.org/10.1007/s11771-021-4735-5

[25] Asszonyi, C., Fülöp, T., Ván, P. "Distinguished rheological models for solids in the framework of a thermodynamical internal variable theory", Continuum Mechanics and Thermodynamics, 27(6), pp. 971–986, 2015.
https://doi.org/10.1007/s00161-014-0392-3

[26] Asszonyi, C., Csatár, A., Fülöp, T. "Elastic, thermal expansion, plastic and rheological processes – theory and experiment", Periodica Polytechnica Civil Engineering, 60(4), pp. 591–601, 2016.
https://doi.org/10.3311/PPci.8628

[27] Gong, F., Ni, Y., Jia, H. "Effects of specimen size on linear energy storage and dissipation laws of red sandstone under uniaxial compression", Bulletin of Engineering Geology and the Environment, 81(9), 386, 2022.
https://doi.org/10.1007/s10064-022-02881-y

[28] Meng, Q., Liu, J., Huang, B., Pu, H., Wu, J., Zhang, Z. "Effects of Confining Pressure and Temperature on the Energy Evolution of Rocks Under Triaxial Cyclic Loading and Unloading Conditions", Rock Mechanics and Rock Engineering 55, pp. 773–798, 2022.
https://doi.org/10.1007/S00603-021-02690-X

[29] Li, Y., Zhao, Y., Tang, J., Zhang, L., Zhou, Y., Zhu, X., Jia, D., Chen, M. "Rock damage evolution model of pulsating fracturing based on energy evolution theory", Energy Science & Engineering, 8(4), pp. 1050–1067, 2020.
https://doi.org/10.1002/ese3.567

[30] Zhang, C., Wang, Y., Ruan, H., Ke, B., Lin, H. "The strain characteristics and corresponding model of rock materials under uniaxial cyclic load/unload compression and their deformation and fatigue damage analysis", Archive of Applied Mechanics, 91, pp. 2481–2496, 2021.
https://doi.org/10.1007/s00419-021-01899-0

[31] Xue, K., Zhao, B., Liu, D., Hu, Y. "Nonlinear creep model of rock in tensile or compressive stress and its parameter identification", Journal of China Coal Society, 36(9), pp. 1440–1445, 2011.
https://doi.org/10.13225/j.cnki.jccs.2011.09.006

[32] Yu, M., Liu, B., Sun, J., Feng, W., Wang, Q. "Study on improved nonlinear viscoelastic-plastic creep model based on the Nishihara model", Geotechnical and Geological Engineering, 38(3), pp. 3203–3214, 2020.
https://doi.org/10.1007/s10706-020-01217-5